Granular Matter (2014) 16:107–114
DOI 10.1007/s10035-013-0472-2

BRIEF COMMUNICATION

Effect of particle shape on domino wave propagation: a perspective from 3D, anisotropic discrete element simulations

G. Lu · J. R. Third · C. R. Müller

Received: 10 April 2013 / Published online: 27 December 2013
© Springer-Verlag Berlin Heidelberg 2013

Abstract A fundamental understanding of the underlying physics of granular systems is not only of academic interest, but is also relevant for industrial applications. One specific aspect that is currently only poorly understood is the effect of particle shape on the dynamics of such systems. In this work the effect of particle shape on domino wave propagation was studied using 3D, anisotropic discrete element simulations. The dominoes were modelled using the three-dimensional super-quadric equation and very good agreement between the intrinsic collision speeds predicted by the simulations and the corresponding experimental data was observed. Furthermore, the influence of particle blockiness on the collision dynamics of dominoes was investigated numerically using particle shapes ranging from ellipsoids to almost cuboid particles. It was found that the intrinsic collision speed increased with increasing particle blockiness. It was also shown that a higher initial contact point favours the transmission of kinetic energy in the direction of the wave propagation, leading to a higher intrinsic collision speed for dominoes of higher blockiness.

Keywords Discrete element model · Anisotropic particles · Granular material · Contact mechanics · Propagating wave

List of symbols

$a,\ b,\ c$	Half lengths of particle principal axes (m)
dt	Time step of DEM simulations (s)
e_{n}	Coefficient of normal restitution (–)
F_{n}	Normal force between colliding particles (N)
F_{t}	Tangential force between colliding particles (N)
g	Gravitational acceleration (m/s^2)
h	Height of contact point (m)
H	Height of domino (m)
k_{n}	Normal spring stiffness (N/m)
$k_{\mathrm{n_{ij}}}$	Effective normal spring stiffness in collision between particles i and j (N/m)
k_{t}	Tangential spring stiffness (N/m)
$k_{\mathrm{t_{ij}}}$	Effective tangential spring stiffness in collision between particles i and j (N/m)
$m,\ n,\ p$	Squareness parameters of particle (–)
m_{ij}	Effective mass in collision between particles i and j (kg)
S	Domino sequence number (–)
t	Simulation time (s)
T	Thickness of domino (m)
u_{c}	Colliding velocity between two dominoes (m/s)
v_n	Relative velocity in normal direction (m/s)
v_t	Relative velocity in tangential direction (m/s)
V	Intrinsic collision speed (m/s)
$x,\ y,\ z$	Coordinates (m)
δ_{n}	Particle overlap (m)
δ_{t}	Tangential displacement (m)
η_{n}	Normal damping factor (–)
η_{t}	Tangential damping factor (–)
λ	Domino spacing (m)
μ	Coefficient of friction (–)
ρ	Particle density (kg/m^3)
θ	Rotation angle of domino (∘)
ϕ	Inclined angle of domino (∘)

G. Lu · J. R. Third · C. R. Müller (✉)
Laboratory of Energy Science and Engineering, Department of Mechanical and Process Engineering, ETH Zürich, Leonhardstrasse 27, 8092 Zurich, Switzerland
e-mail: muelchri@ethz.ch

1 Introduction

At first sight granular systems, i.e. assemblies of macroscopic particles, appear simple. However, under external excitation, e.g. rotation or vibration, a plethora of intriguing phenomena, including segregation or the formation of surface waves, can be observed [1–3]. Granular systems that are frequently encountered in industry or nature are further complicated since they are comprised of non-spherical grains, whereas most numerical and laboratory studies have been restricted to spheres [4]. Thus, the effect of particle shape on the dynamics, and indeed statics [5], of granular systems is currently only poorly understood.

So far, discrete computational methods, such as the discrete element method (DEM), have been employed to provide both macroscopic and microscopic 'measurements' in granular systems [6–10]. Recent developments in the DEM have enabled the modelling of various non-spherical particle shapes [11,12,14–16]. However, model validation and indeed systematic studies critically assessing the effect of particle shape on the dynamics of granular systems are lacking. In this study we utilize the propagation of domino waves to address the above mentioned issues. The toppling of an array of dominoes may produce a propagating wave characterized by successive destabilizing collisions between neighbouring dominoes [17]. If the spacing between neighbouring dominoes is sufficiently large, a so-called intrinsic or natural collision speed can be reached after a transient phase. This intrinsic collision speed is independent of the initial perturbation exerted on the first domino [18] and is predominantly governed by the domino spacing, the sliding friction and the coefficient of restitution of the domino-domino contacts [19,20]. Experimental measurements of the intrinsic speed of colliding dominoes have demonstrated the effectiveness of theoretical predictions based on either the single collision theory [19] or the cooperative group theory [20]. The distinguishing feature of the cooperative group theory is that it considers the effect of the toppled dominoes leaning against each other at the front of the propagating wave. Hence, for the case that the dominoes are narrowly spaced this model provides a more accurate prediction of the intrinsic speed of domino wave propagation compared to the single collision theory.

So far studies concerned with contacts between dominoes and the colliding wave propagation have been restricted to 2D approaches, which are, of course, an over-simplification of reality [21,22]. In those studies the dominoes were modelled as perfect rectangles with sharp corners. In contrast, this study aims to identify the influence of particle blockiness on domino wave propagation using 3D DEM simulations. Particles of non-spherical shape were represented using the 3D super-quadric equation, $viz.\ (x/a)^m + (y/b)^n + (z/c)^p = 1$ (a, b and c are the half lengths of the principal axes and m, n and p are indices controlling the sharpness of the edges). For a specified particle blockiness, we first verified the accuracy of our DEM simulations by using experimental measurements of the intrinsic collision speeds of domino arrays. Subsequently, the blockiness of the dominoes was varied to highlight its influence on the domino wave propagation.

2 Experimental and numerical setup

In the experiments reported here, commercial plastic dominoes with dimensions of 43.2 mm × 21.9 mm × 7.7 mm were used. In total 30 dominoes were arranged in a linear array on a horizontal table. The dominoes were placed on a thin rubber sheet of thickness 1 mm to suppress sliding during the toppling of the dominoes. The spacing, λ, was defined as the 'face-to-face' separation between neighbouring dominoes in the domino array. The dominoes were arranged with their greatest linear dimension ($H = 43.2$ mm) perpendicular to the table and their smallest linear dimension ($T = 7.7$ mm) parallel to λ. The domino wave was initiated by applying an impulse to the first domino and the propagation of the wave was recorded using a high-speed CCD camera (Nikon, 496RC2) using a capture rate of 500 frames per second. The intrinsic collision speed, V, was defined as the speed at which the wave propagates from one domino to the next and was calculated by averaging the speeds obtained from 10 experiments. Here, the moment at which the first domino collides with the second domino was regarded as the starting time. Since it is challenging to identify the exact moment at which two dominoes make contact, the collision speeds reported here have been calculated based on the time required for the domino wave to propagate a distance of 2λ. Calculating the velocity in this way reduces the sensitivity of the results to inaccurately identified contacts.

The coefficients of friction and restitution of the dominoes were measured experimentally. The coefficients of friction for domino-domino and domino-rubber contacts were measured by sliding the edge of a domino on the faces of other dominoes and the surface of the rubber, respectively. A mass of between 195 and 730 g was placed on top of the sliding domino to vary the normal force applied to the sliding contact. The pulling force required to slide the domino at a constant speed was measured using a forcemeter with a maximum scale of 5 N and a resolution of 0.05 N. The average coefficients of friction obtained for the domino-domino and the domino-rubber contacts were 0.11 ± 0.01 and 0.90 ± 0.02, respectively. To measure the coefficient of normal restitution, a domino was dropped from a certain height such that its edge collided with the face of a second domino that was immobilised on a horizontal surface. The initial height of the domino was chosen such that collision speeds in the range of 0.5–1.0 m/s were obtained, i.e. values that approx-

imately cover the linear velocity at which the edge of one domino collides with the face of the other domino during the domino wave propagation considered in this work. The vertical component of the velocity of the falling domino at the contact point was determined immediately before and after the collision with the stationary dominoes using particle image velocimetry (MATPIV) [23]. The coefficient of normal restitution obtained using this method was 0.54 ± 0.10.

In the DEM simulations the dominoes were modelled as 3D super-quadrics. Contact detection and the determination of the contact properties for super-quadric particles were addressed in detail by Lu et al. [12] and will not be repeated here except to describe the force laws adopted in this work. A linear spring and dashpot model was employed to describe the contact mechanics of the particles and attractive forces between colliding particles were prevented. For a pair of colliding particles i and j, the contact force in the normal direction was given by

$$F_{\mathrm{n}} = \max\left(0, k_{\mathrm{n_{ij}}}\delta_{\mathrm{n}} - 2\eta_{\mathrm{n}}\sqrt{m_{\mathrm{ij}}k_{\mathrm{n_{ij}}}}v_{\mathrm{n}}\right) \quad (1)$$

Here δ_{n} is the overlap between the contacting particles, η_{n} is the damping factor in the normal direction, v_{n} is the relative velocity in the normal direction, m_{ij} is the effective mass given by $1/m_{\mathrm{ij}} = 1/m_{\mathrm{i}} + 1/m_{\mathrm{j}}$ and $k_{\mathrm{n_{ij}}}$ is the effective normal stiffness defined as $1/k_{\mathrm{n_{ij}}} = 1/k_{\mathrm{n_i}} + 1/k_{\mathrm{n_j}}$. In the tangential direction, the magnitude of the friction force was restricted by Coulomb's law, such that:

$$F_{\mathrm{t}} = \min\left(\mu k_{\mathrm{n_{ij}}}\delta_{\mathrm{n}}, k_{\mathrm{t_{ij}}}\delta_{\mathrm{t}} - 2\eta_{\mathrm{t}}\sqrt{m_{\mathrm{ij}}k_{\mathrm{t_{ij}}}}v_{\mathrm{t}}\right) \quad (2)$$

where μ is the coefficient of friction, η_{t} is the damping factor in the tangential direction, and v_{t} is the relative velocity in the tangential direction. The tangential displacement was calculated according to $\delta_{\mathrm{t}} = \int v_{\mathrm{t}}\mathrm{d}t$ and the effective tangential stiffness is defined as $1/k_{\mathrm{t_{ij}}} = 1/k_{\mathrm{t_i}} + 1/k_{\mathrm{t_j}}$. Interactions between particles and the bottom surface were modelled in the same way as interactions between particles. The bottom surface was modelled as having an infinite mass and the same normal and tangential stiffnesses as the particles. The time step dt used for the DEM simulations was 5×10^{-5} s, which is approximately one fortieth of the duration of a binary collision between particles. A third order Adams-Bashforth integration scheme was employed to update the particle velocities and positions. The same integration scheme was applied to update the orientation of particles based on the concept of quaternions [13].

To reproduce more accurately the experimental conditions, random deviations were applied to the initial positions of the simulated dominoes in both horizontal directions. The maximum magnitude of these deviations was 0.5 mm. In total 30 dominoes were simulated and 10 independent simulations were performed with different initial angular velocities for the first domino and different initial positions for all the dominoes. The time at which a contact formed between neighbouring dominoes was identified by the DEM code. The dominoes were modelled as super-quadrics with squareness parameters [7 7 7]. Table 1 shows the shapes of the real and simulated dominoes and the mechanical properties of the particles simulated.

Table 1 Shapes of the real and simulated dominoes and the mechanical properties of the particles simulated

Real domino	Super-quadric particle
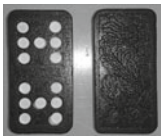	

Mechanical property	Numerical value
Particle density, ρ	631 kg/m^3
Normal spring stiffness, k_{n}	10,000 N/m
Tangential spring stiffness, k_{t}	5,000 N/m
Normal damping factor, η_{n}	0.194
Tangential damping factor, η_{t}	0.194
Coefficient of normal restitution, e_{n}	0.54

3 Results and discussion

Figure 1 shows snapshots of toppling dominoes separated by a spacing of $\lambda/T = 1.8$ obtained from both an experiment and a DEM simulation. Due to the different initial perturbations applied to the two systems, the start time of the snapshots, $t = 0$, is defined as the moment when the eleventh domino forms a contact with the twelfth domino. It can be observed that the characteristics of the domino wave propagation are very similar for the experiment and the simulation. Since the dominoes in this case are separated by a comparatively small spacing, the toppled dominoes lean against each other in the experiment, an effect which was reproduced very accurately in the DEM simulation using super-quadric particles. To compare further the intrinsic collision speeds of the domino arrays, we studied three spacings, i.e. $\lambda/T = 1.0$, 1.8 and 2.6, corresponding to 'face-to-face' separations between neighbouring dominoes of 7.7, 13.86 and 20.02 mm, respectively. A comparison between the intrinsic collision speeds obtained from the experiments and numerical simulations is plotted in Fig. 2. Very good agreement between the simulations and the experiments can be observed in all the cases tested. For the three spacings

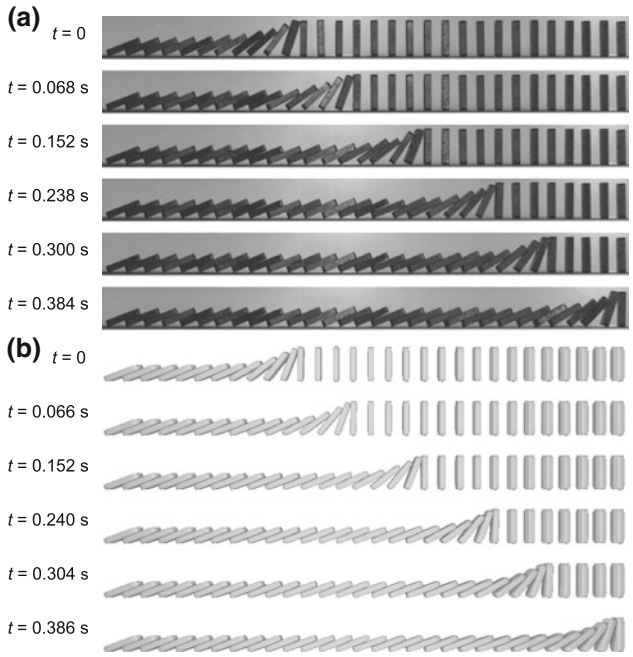

Fig. 1 Snapshots of the toppling of a domino array separated by a spacing of $\lambda/T = 1.8$ (the start time of the snapshots is chosen as the moment when the eleventh domino forms a contact with the twelfth domino): **a** experiment and **b** DEM simulation

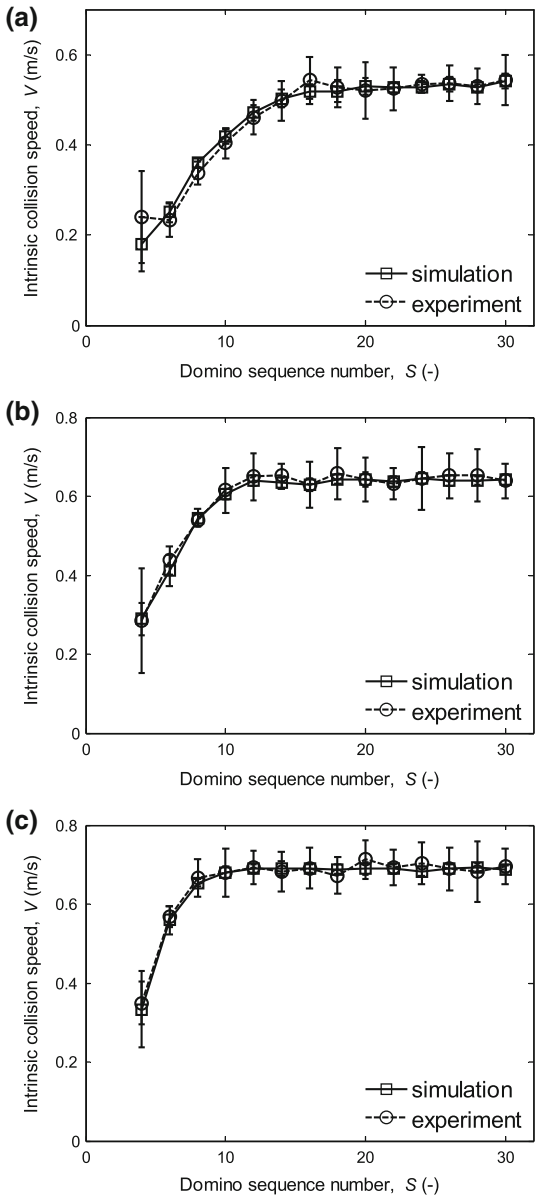

Fig. 2 Comparison of the intrinsic collision speeds of toppling dominoes separated by different spacings obtained using experiments and DEM simulations: **a** $\lambda/T = 1.0$; **b** $\lambda/T = 1.8$; **c** $\lambda/T = 2.6$

studied the propagation speed of the toppling domino wave approached a steady state value. With increasing domino spacing, fewer dominoes were required before the speed of the wave front approached an asymptotic value. On the other hand, the average intrinsic collision speed increased with increasing spacing between the dominoes. These results demonstrate the effectiveness of our 3D DEM simulations in capturing accurately the wave propagation of toppling dominoes.

Apart from the intrinsic collision speed, other physical quantities can be extracted from the experimental data for comparison with the numerical simulations. Here, the inclined angle of an individual domino during collision was chosen. The variation of this angle is plotted as a function of time. To this end, the time at which two dominoes first contact with each other is regarded as the starting moment of record. In the experiments, the inclined angle of a domino was obtained by simply marking two points on the wave-front edge and then calculating the inclination of this linear section with respect to the horizontal (see Fig. 3). The results were averaged for each spacing using 10 different dominoes in the experiments and 100 different dominoes in the simulations. It can be seen in Fig. 4 that the inclined angle of toppling dominoes follows the same trend for the simulations and the experiments. However, a small deviation can be observed. This deviation may be due to the accuracy limitation in the experimental measurement, and also the geometry difference between the experimental and numerical dominoes (see Table 1, a real domino actually has a non-smooth surface).

In order to show the dependence of the wave propagation speed of dominoes with respect to the force models and parameters employed in our DEM simulations, the following more tests were performed. First, the domino-domino friction coefficient was varied using the following values 0.11, 0.2 and 0.5. The friction coefficient between dominoes and the bottom surface was kept fixed at 0.90 to prevent slippage. The results obtained for different spacings are shown in Fig. 5. It can be seen that the domino-domino friction coefficient had a significant influence on the speed of domino

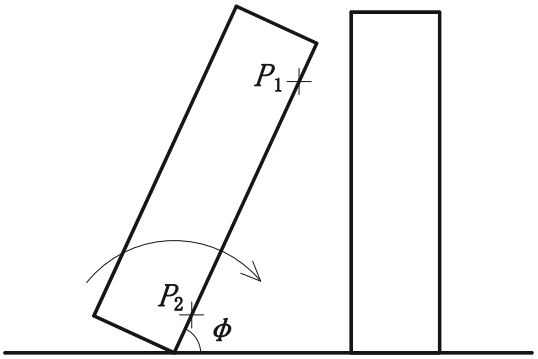

Fig. 3 Schematic diagram showing the wave-front edge and the inclined angle of a toppling domino

wave propagation. The wave speed decreased dramatically with increasing friction coefficient for all domino spacings considered. Furthermore, the different coefficients of restitution for domino-domino and domino-surface collisions were used, viz. $e_n = 0.34$, 0.54 and 0.74. We found that the coefficient of restitution did not have a strong influence on the speed of domino wave propagation. Finally, the influence of the force models employed on the domino wave propagation was studied. We modelled the particle contacts using a simple dynamic friction model, i.e. setting the term $k_{t_{ij}}\delta_t$ [Eq. (2)] to zero. The results were compared with those obtained using the initially implemented force models using domino arrays of different spacings. It was observed that the average intrinsic collision speed for this model was indistinguishable from those shown in Fig. 2.

Previous numerical studies investigating the toppling of dominoes have been restricted to 2D approaches in which a domino was assumed to be a perfect rectangle with sharp edges and vertices. However, it is conceivable that the blockiness of the particles may affect the wave propagation speed since the particle shape influences the contact forces between neighbouring dominoes. Thus, we varied the blockiness of the super-quadric particles by employing squareness parameters of [2 2 2], [3 3 3], [4 4 4], [7 7 7] and [10 10 10], i.e. changing the particle shape from an ellipsoid to an approximate cuboid. To allow the effect of particle blockiness to be isolated, the mass and inertia tensor of the different domino shapes were set to be identical, i.e. equivalent to those of a perfect cuboid with the same linear dimensions. The spacing of the domino array was fixed as $\lambda/T = 1.8$. Again, 10 independent simulations were performed for each domino shape and the same set of random perturbations were applied. The average intrinsic collision speeds obtained are plotted in Fig. 6a. It can be seen that, independent of the blockiness of the particles, a steady state collision speed was reached after the wave front passed approximately 14 dominoes. However, the particle blockiness did affect the magnitude of the intrinsic collision speed, i.e. the intrinsic collision speed increased

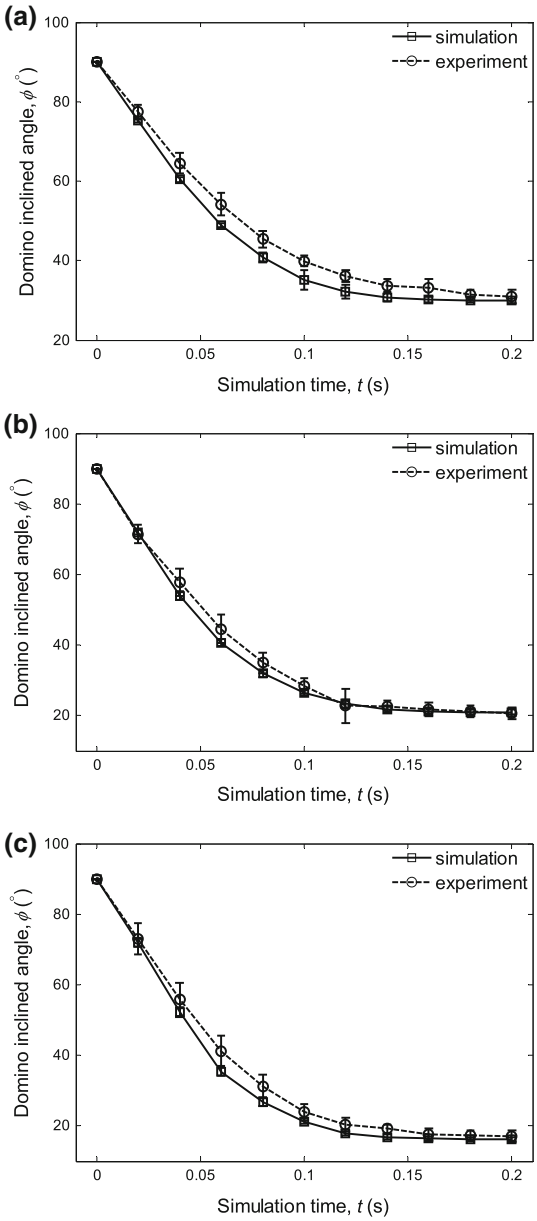

Fig. 4 Comparison of the inclined angle of toppling dominoes separated by different spacings obtained using experiments and DEM simulations: **a** $\lambda/T = 1.0$; **b** $\lambda/T = 1.8$; **c** $\lambda/T = 2.6$

with increasing particle blockiness, in particular for small values of the squareness parameters (see the inset of Fig. 6a). The side and top views of the toppled dominoes using different squareness parameters are shown in Fig. 6b. Significant slip in the transverse direction occurred for particles with relatively small squareness parameters, i.e. in the range [2 2 2] to [4 4 4]. On the other hand, dominoes with squareness parameters [7 7 7] and [10 10 10] did not show any appreciable slip in the transverse direction.

The position of the contact between neighbouring dominoes is believed to influence the transmission of kinetic energy in the direction of the domino array and, thus, the

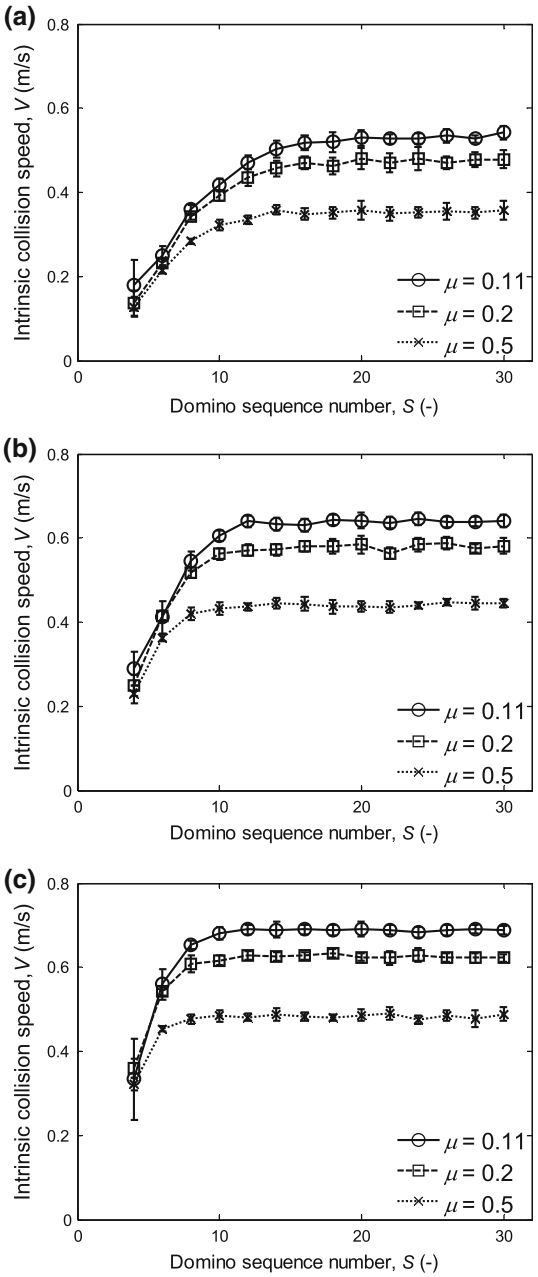

Fig. 5 Comparison of the collision speed of toppling dominoes separated by different spacings with different friction coefficients: **a** $\lambda/T = 1.0$; **b** $\lambda/T = 1.8$; **c** $\lambda/T = 2.6$

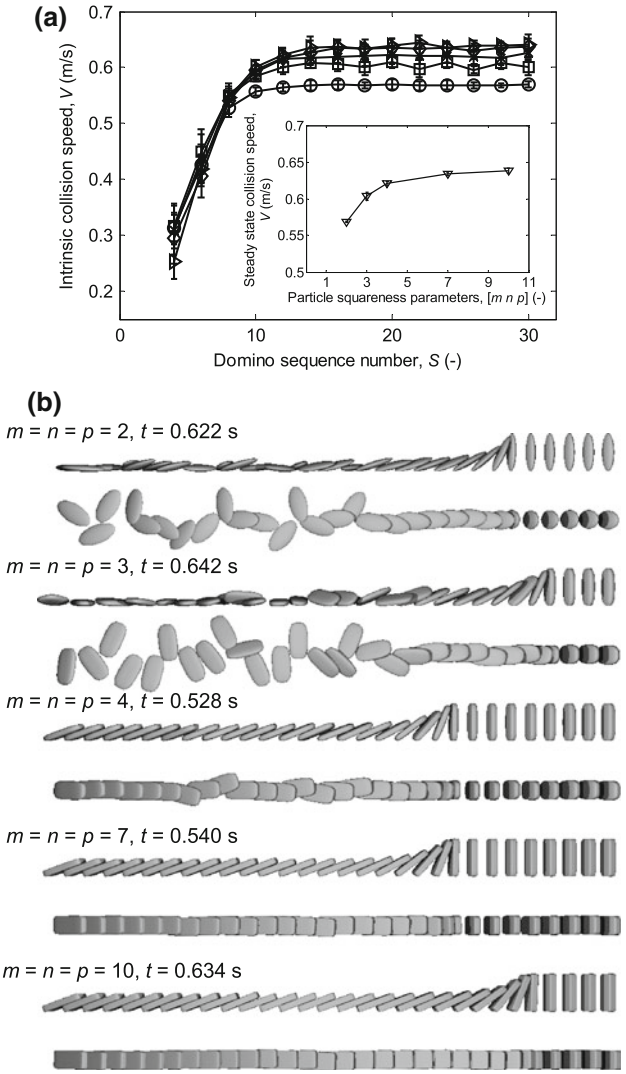

Fig. 6 Effect of particle blockiness on domino wave propagation: **a** intrinsic collision speeds of an array of dominoes as a function of particle blockiness: (◯) $m = n = p = 2$; (□) $m = n = p = 3$; (×) $m = n = p = 4$; (◇) $m = n = p = 7$; (▷) $m = n = p = 10$. In the inset the steady state collision speed is plotted as a function of particle blockiness. **b** Side and top views of the toppled dominoes obtained using super-quadric particles with different blockinesses

wave propagation speed. The heights of the initial contact points between neighbouring dominoes are plotted in Fig. 7a for each domino blockiness considered. It can be seen that the height of the contact point did not change appreciably along the domino array, regardless of whether the intrinsic collision speed had been reached or not. It was also observed that the height of the contact point increased with increasing particle blockiness, following the same trend as the intrinsic collision speed (see the inset of Fig. 7a). Figure 7b illustrates the positions of the contact points for ellipsoidal and cuboid dominoes based on a simple 2D representation. Though the spacing is identical for both particle shapes, the angle through which the ellipsoidal particle rotates prior to collision, θ_1, is larger than the corresponding angle for approximately cuboid particle, θ_2. The difference between θ_1 and θ_2 is due to the higher contact point position of approximately cuboid dominoes and results in a larger projection of the linear velocity, u_c, onto the direction of the domino wave. In other words, dominoes of larger blockiness possess a higher intrinsic collision speed because the kinetic energy is favourably transmitted in the direction of the wave propagation. Our simulations demonstrated that this mechanism is also valid for 3D dominoes.

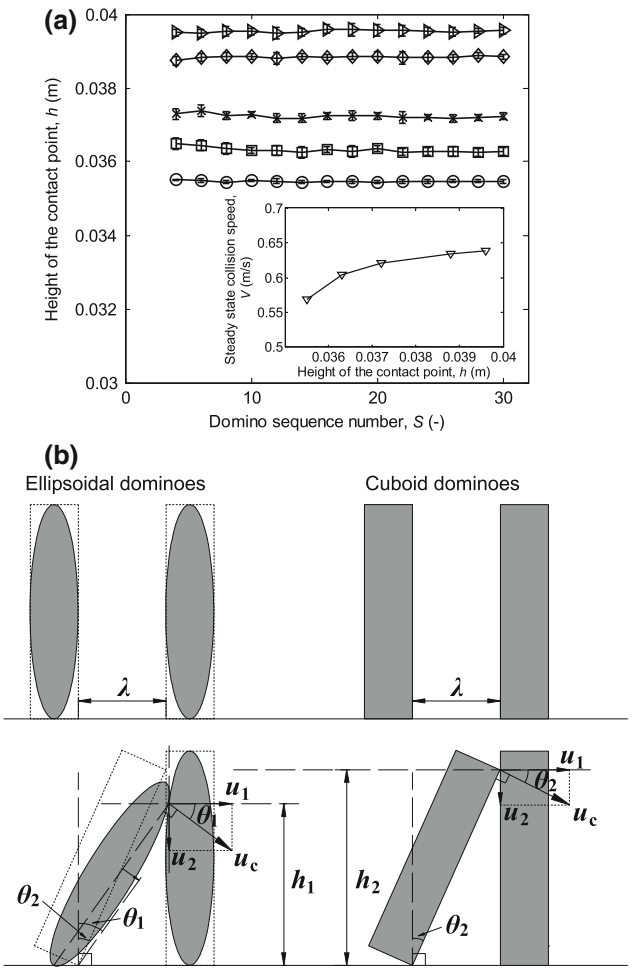

Fig. 7 Effect of the particle blockiness on the characteristics of the domino wave propagation: **a** height of the contact point between neighbouring dominoes as a function of particle blockiness: (◯) $m = n = p = 2$; (□) $m = n = p = 3$; (×) $m = n = p = 4$; (◇) $m = n = p = 7$; (▷) $m = n = p = 10$. The *inset* plots the steady state collision speed as a function of the height of the contact point. **b** 2D schematic diagram showing the effect of the contact position on the transmission of kinetic energy in the direction of the domino wave (for comparison, the dotted rectangles around the ellipsoidal dominoes show the initial contact position between cuboid dominoes)

4 Conclusions

The toppling of dominoes has been studied using 3D DEM simulations. The dominoes were modelled as super-quadric particles, allowing the particle blockiness to be adjusted by varying the squareness parameters of the super-quadric equation. First, the accuracy of the DEM approach to modelling the propagation of domino waves was verified using experiments performed using commercially available dominoes and three different spacings. Very good agreement was observed for the intrinsic collision speeds obtained from the simulations and experiments, demonstrating that anisotropic DEM simulations are an attractive modelling strategy in condensed matter physics. Second, the influence of the particle blockiness on the domino wave propagation was investigated numerically using particles ranging from ellipsoids to approximately cuboid dominoes. It was found that the intrinsic collision speed increased with increasing particle blockiness, an effect which was most pronounced for particle squareness parameters between [2 2 2] and [4 4 4]. Additionally, it was shown that the height of the contact point between neighbouring dominoes increased with increasing particle blockiness, thus favoring the transmission of kinetic energy in the direction of the domino wave. Therefore, at a specified spacing, dominoes of higher blockiness possess a higher intrinsic collision speed, highlighting the importance of particle shape on the physics of granular materials.

Acknowledgments The authors are grateful to the Swiss National Science Foundation (Grant 200021_132657/1) and the China Scholarship Council (Guang Lu) for partial financial support of this work.

References

1. Aranson, I.S., Tsimring, L.S.: Patterns and collective behavior in granular media: theoretical concepts. Rev. Mod. Phys. **78**, 641–692 (2006)
2. Seiden, G., Thomas, P.J.: Complexity, segregation, and pattern formation in rotating-drum flows. Rev. Mod. Phys. **83**, 1323–1365 (2011)
3. Lu, G., Third, J.R., Köhl, M.H., Müller, C.R.: On the occurrence of polygon-shaped patterns in vibrated cylindrical granular beds. Eur. Phys. J. E **35**, 90 (2012)
4. Zhu, H.P., Zhou, Z.Y., Yang, R.Y., Yu, A.B.: Discrete particle simulation of particulate systems: a review of major applications and findings. Chem. Eng. Sci. **63**, 5728–5770 (2008)
5. Hidalgo, R.C., Zuriguel, I., Maza, D., Pagonabarraga, I.: Role of particle shape on the stress propagation in granular packings. Phys. Rev. Lett. **103**, 118001 (2009)
6. Arntz, M.M.H.D., den Otter, W.K., Beeftink, H.H., Boom, R.M., Briels, W.J.: The influence of end walls on the segregation pattern in a horizontal rotating drum. Granul. Matter **15**, 25–38 (2013)
7. Third, J.R., Scott, D.M., Scott, S.A., Müller, C.R.: Effect of periodic boundary conditions on granular motion in horizontal rotating cylinders modelled using the DEM. Granul. Matter **13**, 75–78 (2011)
8. Third, J.R., Scott, D.M., Scott, S.A., Müller, C.R.: Tangential velocity profiles of granular material within horizontal rotating cylinders modelled using the DEM. Granul. Matter **12**, 587–595 (2010)
9. Markauskas, D., Kačianauskas, R.: Investigation of rice grain flow by multi-sphere particle model with rolling resistance. Granul. Matter **13**, 143–148 (2011)
10. Sinnott, M.D., Cleary, P.W.: Vibration-induced arching in a deep granular bed. Granul. Matter **11**, 345–364 (2009)
11. Kyrylyuk, A.V., van de Haar, M.A., Rossi, L., Wouterse, A., Philipse, A.P.: Isochoric ideality in jammed random packings of non-spherical granular matter. Soft Matter **7**, 1671–1674 (2011)
12. Lu, G., Third, J.R., Müller, C.R.: Critical assessment of two approaches for evaluating contacts between super-quadric shaped particles in DEM simulations. Chem. Eng. Sci. **78**, 226–235 (2012)
13. Langston, P.A., Al-Awamleh, M.A., Fraige, F.Y., Asmar, B.N.: Distinct element modelling of non-spherical frictionless particle flow. Chem. Eng. Sci. **59**, 425–435 (2004)

14. Hidalgo, R.C., Kadau, D., Kanzaki, T., Herrmann, H.J.: Granular packings of cohesive elongated particles. Granul. Matter **14**, 191–196 (2012)
15. Guo, Y., Wassgren, C., Ketterhagen, W., Hancock, B., James, B., Curtis, J.: A numerical study of granular shear flows of rod-like particles using the discrete element method. J. Fluid Mech. **713**, 1–26 (2012)
16. Wang, J., Yu, H.S., Langston, P., Fraige, F.: Particle shape effects in discrete element modelling of cohesive angular particles. Granul. Matter **13**, 1–12 (2011)
17. Bert, C.W.: Falling dominoes. SIAM Rev. **28**, 219–224 (1986)
18. Efthimiou, C.J., Johnson, M.D.: Domino waves. SIAM Rev. **49**, 111–120 (2007)
19. Stronge, W.J.: The domino effect: a wave of destabilizing collisions in a periodic array. Proc. R. Soc. Lond. Ser. A **409**, 199–208 (1987)
20. Stronge, W.J., Shu, D.: The domino effect: successive destabilization by cooperative neighbours. Proc. R. Soc. Lond. Ser. A **418**, 155–163 (1988)
21. Hogue, C., Newland, D.: Efficient computer simulation of moving granular particles. Powder Technol. **78**, 51–66 (1994)
22. Fujii, F., Satoh, T., Fukumoto, S.: Dynamic contact mechanics of the domino wave propagation. In: Ambrósio, J., et al. (eds.) 7th EUROMECH Solid Mechanics Conference, pp. 1–13. Lisbon, Portugal (2009)
23. Raffel, M., Willert, C.E., Kompenhans, J.: Particle Image Velocimetry: A Practical Guide. Springer, Berlin (1998)
24. Wassgren, C.R.: Vibration of Granular Materials. PhD dissertation, California Institute of Technology, Pasadena, California, USA (1997)